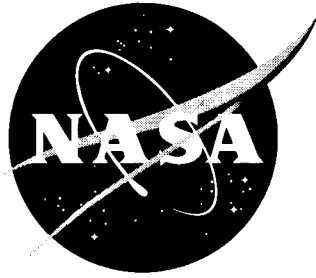# A Variational Principle for Reconstruction of Elastic Deformations in Shear Deformable Plates and Shells

Alexander Tessler
Langley Research Center, Hampton, Virginia

Jan L. Spangler
Lockheed Martin Aeronautics Company, Hampton, Virginia

Since its founding, NASA has been dedicated to the advancement of aeronautics and space science. The NASA Scientific and Technical Information (STI) Program Office plays a key part in helping NASA maintain this important role.

The NASA STI Program Office is operated by Langley Research Center, the lead center for NASA's scientific and technical information. The NASA STI Program Office provides access to the NASA STI Database, the largest collection of aeronautical and space science STI in the world. The Program Office is also NASA's institutional mechanism for disseminating the results of its research and development activities. These results are published by NASA in the NASA STI Report Series, which includes the following report types:

- TECHNICAL PUBLICATION. Reports of completed research or a major significant phase of research that present the results of NASA programs and include extensive data or theoretical analysis. Includes compilations of significant scientific and technical data and information deemed to be of continuing reference value. NASA counterpart of peer-reviewed formal professional papers, but having less stringent limitations on manuscript length and extent of graphic presentations.

- TECHNICAL MEMORANDUM. Scientific and technical findings that are preliminary or of specialized interest, e.g., quick release reports, working papers, and bibliographies that contain minimal annotation. Does not contain extensive analysis.

- CONTRACTOR REPORT. Scientific and technical findings by NASA-sponsored contractors and grantees.

- CONFERENCE PUBLICATION. Collected papers from scientific and technical conferences, symposia, seminars, or other meetings sponsored or co-sponsored by NASA.

- SPECIAL PUBLICATION. Scientific, technical, or historical information from NASA programs, projects, and missions, often concerned with subjects having substantial public interest.

- TECHNICAL TRANSLATION. English-language translations of foreign scientific and technical material pertinent to NASA's mission.

Specialized services that complement the STI Program Office's diverse offerings include creating custom thesauri, building customized databases, organizing and publishing research results ... even providing videos.

For more information about the NASA STI Program Office, see the following:

- Access the NASA STI Program Home Page at *http://www.sti.nasa.gov*

- E-mail your question via the Internet to help@sti.nasa.gov

- Fax your question to the NASA STI Help Desk at (301) 621-0134

- Phone the NASA STI Help Desk at (301) 621-0390

- Write to:
  NASA STI Help Desk
  NASA Center for AeroSpace Information
  7121 Standard Drive
  Hanover, MD 21076-1320
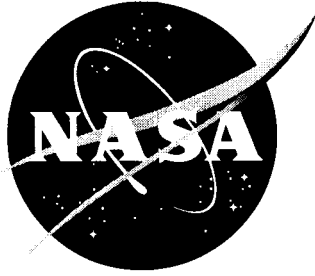
A Variational Principle for Reconstruction of Elastic Deformations in Shear Deformable Plates and Shells

Alexander Tessler
Langley Research Center, Hampton, Virginia

Jan L. Spangler
Lockheed Martin Aeronautics Company, Hampton, Virginia

August 2003

A Variational Principle for Reconstruction of Elastic Deformations in Shear Deformable Plates and Shells

Alexander Tessler

NASA Langley Research Center, Hampton, VA 23681

Jan L. Spangler

Lockheed Martin Aeronautics Company
NASA Langley Research Center, Hampton, VA 23681

ABSTRACT

A variational principle is formulated for the inverse problem of full-field reconstruction of three-dimensional plate/shell deformations from experimentally measured surface strains. The formulation is based upon the minimization of a least squares functional that uses the complete set of strain measures consistent with linear, first-order shear-deformation theory. The formulation, which accommodates for transverse shear deformation, is applicable for the analysis of thin and moderately thick plate and shell structures. The main benefit of the variational principle is that it is well suited for C^0-continuous displacement finite element discretizations, thus enabling the development of robust algorithms for application to complex civil and aeronautical structures. The methodology is especially aimed at the next generation of aerospace vehicles for use in real-time structural health monitoring systems.

1. INTRODUCTION

Structural health monitoring is recognized as a key technology that is needed for the development of the next generation of aerospace vehicles. The principal purpose is real-time monitoring of the aerospace vehicle structural integrity using a network of in-flight sensors that measure quantities such as temperature and strain. Using such measurements, general structural deformations need to be identified, together with the material or structural failure modes. A great deal of recent work on structural health monitoring can be found in [1, 2].

Real-time reconstruction of full-field structural displacements is also essential technology for providing feedback to the actuation and control systems for the morphed wings of the next generation aircraft. It is envisioned that load-carrying structural components will be instrumented with a network of sensors measuring surface strains (e.g., fiber optic sensors with Bragg gratings). The reconstruction of the displacement vector at every material point of the structure (i.e., full-field reconstruction) from a set of strain measurements represents an inverse problem. Knowing a detailed state of structural deformations also implies that other essential response quantities such as stress and failure criteria can be assessed.

Inverse problems are ill posed in the sense that they do not necessarily satisfy conditions of existence, uniqueness, and stability. Concerning the issue of uniqueness, there may be an infinite arrangement of strain sensors, the values of measured strains, initial and boundary conditions that correspond to nearly the same displacement response. Instabilities are generally manifested by arbitrarily small disturbances in the measured data (such as strains) that may cause great changes in the solution (displacements). Tikhonov and Arsenin [3] discussed a general method of improving robustness of mathematical algorithms by enforcing additional physical (regularity) constraints by way of a specially constructed regularization term that ensures a certain degree of smoothness of the approximate solution. The majority of the inverse algorithms today use some type of Tikhonov s regularization.

Although many types of inverse problems and their applications are addressed in the literature (e.g., refer to [4-7] and references therein), few deal with the problem of the reconstruction of three-dimensional deformations of bending structures in general. Even fewer papers focus on the large-scale computations associated with high-fidelity plate and shell models - the kind of structures that are most common in modern aerospace design. Almost exclusively, various forms of least-squares approaches have been used. Bogert et al. [8] used a modal transformation method that allows the development of suitable strain-to-displacement transformations. Their approach makes use of a large number of natural vibration modes. When applied to high-fidelity finite element models, however, the method necessitates a computationally intensive eigenvalue analysis that requires a detailed description of the elastic and inertial material properties. Jones et al. [9] used a least-squares approach to solve the inverse problem of reconstructing deformations of a cantilever plate, where the axial strain was fitted with a cubic polynomial. The strain field was then integrated with the use of approximate boundary conditions at the clamped end to obtain plate deflections according to classical bending assumptions. Recently, taking a view on high-fidelity modeling of aeronautical structures, Shkarayev et al. [10, 11] used a two-step solution procedure. The first step involves the structural analysis of a plate/shell finite element model, and the second step applies a least-squares algorithm. The methodology requires reconstructing the applied loading first, which then leads to the displacements.

It needs to be stated that none of the existing reconstruction methods has been applied and validated on high-fidelity plate and shell structural models. Moreover, many of these methods are restricted, by virtue of the inherent assumptions, to static loads and linear deformations, and cannot be modified to deal with dynamic and nonlinear deformations. None of these methods satisfies the requirements of a viable structural health-monitoring algorithm. These requirements are real-time (fast) computations, robustness, and the ability to model high-fidelity plate and shell structures spanning a variety of response regimes.

This paper will discuss a variational principle that provides the mathematical framework from which a robust Inverse Finite Element Method (I-FEM) can be developed. The problem of interest is the reconstruction of structural deformations from experimentally measured strains. A formulation will be presented that is based upon the minimization of a least squares functional that uses the complete set of strain measures of a linear, first-order plate theory including the membrane, bending, and transverse shear deformations. The error functional uses the least-squares-difference terms comprised of the strains that are expressed in terms of the displacements and the corresponding strains that are measured experimentally. All strain-displacement relations are enforced explicitly whereas the analytical and measured strains are matched in the least-squares sense. By virtue of these assumptions, all strain compatibility relations are explicitly satisfied. The degree of enforcement of the transverse shear strains to the

corresponding strain data is controlled by a penalty parameter. When the measured strains are smoothed a priori, it is shown that an inverse boundary-value problem can be established, giving rise to a set of Euler equations and the corresponding boundary conditions. A correspondence between a direct plate analysis and an inverse one is established by way of an analytical plate-bending example. This paper will conclude with guidelines for developing the inverse finite element method by discretization with C^0-continuous displacement interpolation functions. The advantages of this new inverse finite element method, particularly in relation to high fidelity (large-scale) linear, nonlinear and dynamics problems of plate and shell structural models, will also be discussed.

2. INVERSE VARIATIONAL FORMULATION

Consider an arbitrary panel depicted in Figure 1 that is defined in a three-dimensional Cartesian coordinate frame (x, y, z) on the domain of the form:

$$\Omega = \left\{ (x, y, z) \subset R^3; \ z \in [-t, t], \ (x, y) \in A \subset R^2 \right\}$$

where $2t$ is the panel thickness, $z = 0$ denotes its middle plane position, A denotes the area of the middle plane, and s is its boundary. The panel is subjected to external loads that may include the in-plane and out-of-plane components, and is restrained against rigid body motion.

Either conventional strain rosettes or fiber Bragg-grating optic sensors obtain the information about the state of strain in the panel. Strains are measured on the top and bottom panel surfaces, $\mathbf{x}_i = (x_i, y_i, \pm t)$ $(i = 1, N)$. It is implied that all three of the strain components are co-located, i.e., they are measured at the same point $\mathbf{x}_i$. The restriction of co-located strain components can be removed if curve-fitting or smoothing methods are used to map the discrete strain measurements onto smooth and continuous functions (refer to the discussion in section 2.5). The measured strains are denoted as $(\varepsilon_{xx}^+, \ \varepsilon_{yy}^+, \ \gamma_{xy}^+)_i$ and $(\varepsilon_{xx}^-, \ \varepsilon_{yy}^-, \ \gamma_{xy}^-)_i$, where superscripts $+$ and $-$ represent the top and bottom surface locations. Although more general conditions may be applicable, it is assumed that the panel is initially flat and its structural response is linear.

The inverse problem at hand is the reconstruction of the three-dimensional deformations of plate and shell structures based upon the experimentally measured discrete surface strains and well-defined boundary restraints. The actual loads that cause the deformations are unknown; however, their influences are represented in the measured strains. The precise nature of the admissible boundary conditions and the degree of smoothness of the solution displacements will be established from a variational principle.

2.1 Kinematic relations

The deformations of plate and flat shell structures are assumed to correspond to the well-established assumptions of first-order, shear-deformation theory. Accordingly, the displacement of any material point of the shell can be described by the three components of the displacement

vector as (refer to Figure 1 and [12-14]):

$$u_x(x,y,z) = u + z\,\theta_y, \quad u_y(x,y,z) = v + z\,\theta_x, \quad u_z(x,y,z) = w \qquad (1)$$

where $u = u(x,y)$ and $v = v(x,y)$ are the mid-plane displacements in the x and y directions, respectively; $\theta_x = \theta_x(x,y)$ and $\theta_y = \theta_y(x,y)$ are the rotations of the normal about the negative x and positive y axes, respectively; and $w = w(x,y)$ is the deflection variable which is a weighted-average of the $u_z(x,y,z)$ displacement across the shell thickness.

Using Eqs. (1), the strain-displacement relations of linear elasticity theory give rise to the strain expressions

$$\begin{Bmatrix} \varepsilon_{xx} \\ \varepsilon_{yy} \\ \gamma_{xy} \end{Bmatrix} = \begin{Bmatrix} \varepsilon_{x0} \\ \varepsilon_{y0} \\ \gamma_{xy0} \end{Bmatrix} + z \begin{Bmatrix} \kappa_{x0} \\ \kappa_{y0} \\ \kappa_{xy0} \end{Bmatrix} \equiv \mathbf{e(u)} + z\,\mathbf{k(u)} \qquad (2)$$

where the in-plane strain measures associated with the stretching of the middle surface are given as

$$\mathbf{e(u)} \equiv \begin{Bmatrix} \varepsilon_{x0} \\ \varepsilon_{y0} \\ \gamma_{xy0} \end{Bmatrix} = \begin{bmatrix} \dfrac{\partial}{\partial x} & 0 & 0 & 0 & 0 \\ 0 & \dfrac{\partial}{\partial y} & 0 & 0 & 0 \\ \dfrac{\partial}{\partial y} & \dfrac{\partial}{\partial x} & 0 & 0 & 0 \end{bmatrix} \begin{Bmatrix} u \\ v \\ w \\ \theta_x \\ \theta_y \end{Bmatrix} \equiv \mathbf{L}_\varepsilon\,\mathbf{u} \qquad (3)$$

and the bending curvatures have the form

$$\mathbf{k(u)} \equiv \begin{Bmatrix} \kappa_{x0} \\ \kappa_{y0} \\ \kappa_{xy0} \end{Bmatrix} = \begin{bmatrix} 0 & 0 & 0 & 0 & \dfrac{\partial}{\partial x} \\ 0 & 0 & 0 & \dfrac{\partial}{\partial y} & 0 \\ 0 & 0 & 0 & \dfrac{\partial}{\partial x} & \dfrac{\partial}{\partial y} \end{bmatrix} \begin{Bmatrix} u \\ v \\ w \\ \theta_x \\ \theta_y \end{Bmatrix} \equiv \mathbf{L}_\kappa\,\mathbf{u} \qquad (4)$$

The transverse shear strains can also be expressed in terms of the same five kinematic variables as

$$\mathbf{g(u)} \equiv \begin{Bmatrix} \gamma_{xz0} \\ \gamma_{yz0} \end{Bmatrix} = \begin{bmatrix} 0 & 0 & \dfrac{\partial}{\partial x} & 0 & 1 \\ 0 & 0 & \dfrac{\partial}{\partial y} & 1 & 0 \end{bmatrix} \begin{Bmatrix} u \\ v \\ w \\ \theta_x \\ \theta_y \end{Bmatrix} \equiv \mathbf{L}_\gamma\,\mathbf{u} \qquad (5)$$

2.2 Compatibility conditions

Consistent with first-order, shear-deformation theory, the eight independent strain measures, ε_{x0}, ε_{y0}, γ_{xy0}, κ_{x0}, κ_{y0}, κ_{xy0}, γ_{xz0}, and γ_{yz0}, are interrelated through the four equations of compatibility that can be written as

$$\frac{\partial^2}{\partial x \partial y}\gamma_{xy0} = \frac{\partial^2}{\partial y^2}\varepsilon_{x0} + \frac{\partial^2}{\partial x^2}\varepsilon_{y0}$$

$$\frac{\partial^2}{\partial x \partial y}\kappa_{xy0} = \frac{\partial^2}{\partial y^2}\kappa_{x0} + \frac{\partial^2}{\partial x^2}\kappa_{y0}$$

$$2\frac{\partial}{\partial y}\kappa_{x0} = \frac{\partial}{\partial x}\left(\kappa_{xy0} - \frac{\partial}{\partial x}\gamma_{yz0} + \frac{\partial}{\partial y}\gamma_{xz0}\right) \tag{6}$$

$$2\frac{\partial}{\partial x}\kappa_{y0} = \frac{\partial}{\partial y}\left(\kappa_{xy0} - \frac{\partial}{\partial y}\gamma_{xz0} + \frac{\partial}{\partial x}\gamma_{yz0}\right)$$

These equations serve as <u>integrability conditions</u> leading to a compatible set of only five independent displacement variables u, v, w, θ_x, and θ_y.

2.3 Discrete strain measures computed from experimental data

Evaluating Eqs. (2) at the discrete locations $(x_i, y_i, z = \pm t)$, where the strains are measured, the relationships between the measured surface strains and the reference plane strains and curvatures can be readily determined as

$$\mathbf{e}_i^\varepsilon \equiv \begin{Bmatrix} \varepsilon_{x0}^\varepsilon \\ \varepsilon_{y0}^\varepsilon \\ \gamma_{xy0}^\varepsilon \end{Bmatrix}_i = \frac{1}{2}\left(\begin{Bmatrix} \varepsilon_{xx}^+ \\ \varepsilon_{yy}^+ \\ \gamma_{xy}^+ \end{Bmatrix}_i + \begin{Bmatrix} \varepsilon_{xx}^- \\ \varepsilon_{yy}^- \\ \gamma_{xy}^- \end{Bmatrix}_i\right) \quad (i = 1, N) \tag{7}$$

$$\mathbf{k}_i^\varepsilon \equiv \begin{Bmatrix} \kappa_{x0}^\varepsilon \\ \kappa_{y0}^\varepsilon \\ \kappa_{xy0}^\varepsilon \end{Bmatrix}_i = \frac{1}{2t}\left(\begin{Bmatrix} \varepsilon_{xx}^+ \\ \varepsilon_{yy}^+ \\ \gamma_{xy}^+ \end{Bmatrix}_i - \begin{Bmatrix} \varepsilon_{xx}^- \\ \varepsilon_{yy}^- \\ \gamma_{xy}^- \end{Bmatrix}_i\right) \quad (i = 1, N) \tag{8}$$

In the above equations, the ε superscript is used to signify the existence of experimental error in the strain measurements and, hence, in $\mathbf{e}_i^\varepsilon$ and $\mathbf{k}_i^\varepsilon$.

2.4 Deformation modes

The shell whose material properties are symmetric with respect to the mid-plane may undergo the following deformation modes: (a) Under transverse loading, the resulting deformations are due to bending only. In this case, the strain distribution is anti-symmetric with respect to the mid-plane. Hence, since the mid-plane does not stretch $(e = 0)$, the surface strain values at a given $(x_i, y_i, \pm t)$ location differ only by a sign. Therefore, the strains need only be measured on one of the bounding surfaces, e.g., $(z = t)$. (b) Under purely in-plane loading, the shell is undergoing only stretching deformations, the strains are uniform through the thickness $(k = 0)$. In this case, a single surface strain measurement is also sufficient. Finally, (c) In a completely general case, exhibiting both stretching and bending, both the top and bottom surface strains need to be measured.

2.5 Role of curve fitting and smoothing techniques

Experimental strain data can be treated analytically by applying curve fitting or smoothing techniques [15]. In this manner, the six strain measures in Eqs. (7) and (8) can be represented as continuous functions that are defined everywhere in the reference mid-plane of the shell. The vectors containing the curve-fitted or smoothed mid-plane strains and curvatures will henceforth be denoted as e^ε and k^ε, where the i subscript is omitted to differentiate these continuous quantities from the discrete ones.

A recently developed smoothing procedure, by Tessler and co-workers [16-17], called the Smoothing Element Analysis (SEA), can be used to minimize the experimental error in each strain component. The method, which is based upon finite element approximations, yields a smoothed (strain) field that is represented by a piece-wise, nearly C^1-continuous polynomial function having C^0-continuous first-order derivatives. The benefit of the latter aspect is that it enables the first-order derivatives of k^ε to be used in computing the transverse shear strains g^ε. The method involves the use of appropriate equilibrium equations of first-order theory. Hence, for problems where shear deformation is important, SEA-based treatment of strain data may be desirable. The mathematical details for determining the transverse shear strains g^ε will be discussed in a separate report.

2.6 Variational statement

A least-squares variational principle is formulated enabling the development of robust algorithms for solving the inverse problem of reconstruction of three-dimensional deformations of plate, shell and general built-up structures from experimental strain measurements. For the case when the measured strain data can be represented with continuous functions, the minimization of the error functional results in an inverse boundary value problem described by Euler equations and consistent boundary conditions. The variational principle can also be discretized in a piece-wise continuous manner by using the displacement finite element method.

Accounting for the membrane, bending and transverse shear deformations, an extremum of a least squares functional is sought for a fixed value of a scalar penalty parameter $\lambda > 0$

$$\Phi^\lambda(\mathbf{u}) = \left\| \mathbf{e}(\mathbf{u}) - \mathbf{e}^\varepsilon \right\|^2 + \left\| \mathbf{k}(\mathbf{u}) - \mathbf{k}^\varepsilon \right\|^2 + \lambda \left\| \mathbf{g}(\mathbf{u}) - \mathbf{g}^\varepsilon \right\|^2 \tag{9}$$

where the squared norms can be written in the form of the normalized Euclidean norms as

$$\left\| \mathbf{e}(\mathbf{u}) - \mathbf{e}^\varepsilon \right\|^2 \equiv \frac{1}{N} \sum_{i=1}^{N} \left[\mathbf{e}(\mathbf{u})_i - \mathbf{e}_i^\varepsilon \right]^2$$

$$\left\| \mathbf{k}(\mathbf{u}) - \mathbf{k}^\varepsilon \right\|^2 \equiv \frac{A}{N} \sum_{i=1}^{N} \left[\mathbf{k}(\mathbf{u})_i - \mathbf{k}_i^\varepsilon \right]^2 \tag{10}$$

$$\left\| \mathbf{g}(\mathbf{u}) - \mathbf{g}^\varepsilon \right\|^2 \equiv \frac{1}{N} \sum_{i=1}^{N} \left[\mathbf{g}(\mathbf{u})_i - \mathbf{g}_i^\varepsilon \right]^2$$

where the following notation has been used $(\bullet)_i \equiv (\bullet)_{\mathbf{x}=\mathbf{x}_i}$.

The first term in Eq. (9) corresponds to the membrane deformations whereas the second and third terms pertain to the bending response. The latter two terms are coupled; however, they are decoupled from the first term. This is fully consistent with the assumptions of first-order shear-deformation theory for linear, planar shells possessing a mid-plane material symmetry.

In Eqs. (10), the normalization parameter, N, which represents the number of strain measurement locations, factors out. In a finite element (piece-wise continuous) formulation, however, N is replaced by its counterpart at the finite element level, n (the number of strain measurements within a finite element) which, generally, does not factor out since individual elements may have different number of sensors within them.

Furthermore, an assumption in Eqs. (10) is that $\mathbf{g}_i^\varepsilon$ can be calculated from the strain measurements. A candidate method for determining these quantities was briefly mentioned in Section 2.5. In the majority of practical engineering problems and particularly in the deformation of thin shells, the $\mathbf{g}_i^\varepsilon$ contributions are much smaller compared to the curvatures, $\mathbf{k}_i^\varepsilon$. Hence, the $\mathbf{g}_i^\varepsilon$ contributions can be safely omitted in the formulation. The third equation of Eqs. (10) will then be replaced by the L_2 squared norm

$$\left\| \mathbf{g}(\mathbf{u}) \right\|^2 \equiv \frac{1}{A} \int_A \mathbf{g}(\mathbf{u})^2 \, dx \, dy \tag{11}$$

If the raw strain data is initially processed by means of curve fitting or smoothing procedures, such that continuous experimental strain measures become available, then the error functional

in Eq.(9) can be conveniently redefined in terms of the dimensionless L_2 squared norms given as

$$\left\| \mathbf{e}(\mathbf{u}) - \mathbf{e}^\varepsilon \right\|^2 \equiv \frac{1}{A} \int_A \left[\mathbf{e}(\mathbf{u}) - \mathbf{e}^\varepsilon \right]^2 dx \, dy$$

$$\left\| \mathbf{k}(\mathbf{u}) - \mathbf{k}^\varepsilon \right\|^2 \equiv \int_A \left[\mathbf{k}(\mathbf{u}) - \mathbf{k}^\varepsilon \right]^2 dx \, dy \qquad (12)$$

$$\left\| \mathbf{g}(\mathbf{u}) - \mathbf{g}^\varepsilon \right\|^2 \equiv \frac{1}{A} \int_A \left[\mathbf{g}(\mathbf{u}) - \mathbf{g}^\varepsilon \right]^2 dx \, dy$$

where the $(\bullet)^\varepsilon$ quantities represent the continuous experimental strain measures. These definitions of the error norms enable the derivation of Euler equations and variationally consistent boundary conditions that together describe an inverse boundary value problem.

The error functional in Eq. (9) makes use of the complete set (eight) of the strain measures that is turn satisfy the strain compatibility equations, Eqs. (6). This means that the error functional is fully regularized since all displacement and strain compatibility conditions are enforced through the assumptions (3)-(5).

The penalty parameter λ serves the role of balancing the degree of correlation between the measured strains and their analytical representations, i.e., λ controls the enforcement of the transverse shear and curvature constraints

Transverse shear constraints

$$\mathbf{g}(\mathbf{u}) - \mathbf{g}_i^\varepsilon \rightarrow 0 \qquad (13)$$

Curvature constraints

$$\mathbf{k}(\mathbf{u}) - \mathbf{k}_i^\varepsilon \rightarrow 0 \qquad (14)$$

This is because the two types of strain measures are inherently coupled. Since the raw strain measurements contribute directly to the curvatures (as well as the membrane strains), and the curvature values are commonly several orders of magnitude greater than the shear strains, the value of λ needs to be much smaller than unity, with unity representing the weighting parameter on the curvature term. It may also be argued that since the $\mathbf{g}_i^\varepsilon$ contributions can only be determined through an additional mathematical treatment of the raw data, which may require differentiation of the curvature terms as was suggested earlier, the accuracy of the determined $\mathbf{g}_i^\varepsilon$ strains will necessarily be less than the accuracy of the curvature terms. This again supports the notion that the curvature constraints should be enforced much closer than the shear constraints, thus suggesting that $\lambda \ll 1$.

2.7 Euler equations and boundary conditions

Taking the error functional in Eq. (9) defined in terms of the L_2 norms in Eqs. (12), and setting the first variation of the error functional to zero,

$$\delta \Phi^\lambda(\mathbf{u}) = 0 \qquad (15)$$

where the five displacement (kinematic) variables are being varied, and integrating by parts, results in five Euler equations and a set of consistent boundary conditions.

The boundary conditions are defined on the two parts of the cylindrical shell boundary surrounding the mid-plane (refer to Figure 2): (i) C_u is the part of the mid-plane boundary where the displacements $u^\varepsilon, v^\varepsilon, w^\varepsilon$, θ_x^ε, and θ_y^ε are prescribed (experimentally measured), and (ii) C_ε is the part of the boundary where the strain variables $\varepsilon_{xo}^\varepsilon, \varepsilon_{yo}^\varepsilon, ..., \gamma_{yzo}^\varepsilon$ are prescribed (measured), and v is the outward normal to C_ε defined by its direction cosines,

$$\left[v_x, \quad v_y\right] = \left[cos(x,v), \quad cos(y,v)\right] \tag{16}$$

In practice, it is envisioned that only the displacement boundary conditions on C_u can be measured with sufficient accuracy, and no attempt will be made to determine the strains $\varepsilon_{xo}^\varepsilon, \varepsilon_{yo}^\varepsilon, ..., \gamma_{yzo}^\varepsilon$ along the C_ε boundary. From a viewpoint of finite element approximations, this is directly equivalent with a standard displacement formulation, where only the kinematic (displacement) boundary conditions are required and not the natural (kinetic) boundary conditions.

2.7.1 Euler equations due to membrane response

$$\begin{bmatrix} \dfrac{\partial^2}{\partial x^2} + \dfrac{\partial^2}{\partial y^2} & \dfrac{\partial^2}{\partial x \partial y} \\[3mm] \dfrac{\partial^2}{\partial x \partial y} & \dfrac{\partial^2}{\partial x^2} + \dfrac{\partial^2}{\partial y^2} \end{bmatrix} \begin{Bmatrix} u \\ v \end{Bmatrix} = \begin{Bmatrix} \varepsilon_{xo,x}^\varepsilon + \gamma_{xyo,y}^\varepsilon \\ \varepsilon_{yo,y}^\varepsilon + \gamma_{xyo,x}^\varepsilon \end{Bmatrix} \quad \text{on } A \tag{17.1}$$

Kinematic boundary conditions

$$\begin{Bmatrix} u \\ v \end{Bmatrix} = \begin{Bmatrix} u^\varepsilon \\ v^\varepsilon \end{Bmatrix} \quad \text{on } C_u \tag{17.2}$$

Natural boundary conditions

$$\begin{bmatrix} v_x \dfrac{\partial}{\partial x} + v_y \dfrac{\partial}{\partial y} & v_y \dfrac{\partial}{\partial x} \\[3mm] v_x \dfrac{\partial}{\partial y} & v_x \dfrac{\partial}{\partial x} + v_y \dfrac{\partial}{\partial y} \end{bmatrix} \begin{Bmatrix} u \\ v \end{Bmatrix} = \begin{Bmatrix} v_x \varepsilon_{xo}^\varepsilon + v_y \gamma_{xyo}^\varepsilon \\ v_y \varepsilon_{yo}^\varepsilon + v_x \gamma_{xyo}^\varepsilon \end{Bmatrix} \quad \text{on } C_\varepsilon \tag{17.3}$$

2.7.2 Euler equations due to bending response

$$\begin{bmatrix} \dfrac{\partial^2}{\partial x^2}+\dfrac{\partial^2}{\partial y^2} & \dfrac{\partial}{\partial y} & \dfrac{\partial}{\partial x} \\[2ex] -\dfrac{\lambda}{A}\dfrac{\partial}{\partial y} & \dfrac{\partial^2}{\partial x^2}+\dfrac{\partial^2}{\partial y^2}-\dfrac{\lambda}{A} & \dfrac{\partial^2}{\partial x\partial y} \\[2ex] -\dfrac{\lambda}{A}\dfrac{\partial}{\partial x} & \dfrac{\partial^2}{\partial x\partial y} & \dfrac{\partial^2}{\partial x^2}+\dfrac{\partial^2}{\partial y^2}-\dfrac{\lambda}{A} \end{bmatrix}\begin{Bmatrix} w \\ \theta_x \\ \theta_y \end{Bmatrix} = \begin{Bmatrix} \gamma^{\varepsilon}_{xzo,x}+\gamma^{\varepsilon}_{yzo,y} \\[1ex] \kappa^{\varepsilon}_{yo,y}+\kappa^{\varepsilon}_{xyo,x}-\dfrac{\lambda}{A}\gamma^{\varepsilon}_{yzo} \\[1ex] \kappa^{\varepsilon}_{xo,x}+\kappa^{\varepsilon}_{xyo,y}-\dfrac{\lambda}{A}\gamma^{\varepsilon}_{xzo} \end{Bmatrix} \quad \text{on } A \quad (18.1)$$

Kinematic boundary conditions

$$\begin{Bmatrix} w \\ \theta_x \\ \theta_y \end{Bmatrix} = \begin{Bmatrix} w^{\varepsilon} \\ \theta^{\varepsilon}_x \\ \theta^{\varepsilon}_y \end{Bmatrix} \quad \text{on } C_u \tag{18.2}$$

Natural boundary conditions

$$\begin{bmatrix} v_x\dfrac{\partial}{\partial x}+v_y\dfrac{\partial}{\partial y} & v_y & v_x \\[2ex] 0 & v_y\dfrac{\partial}{\partial x} & v_x\dfrac{\partial}{\partial x}+v_y\dfrac{\partial}{\partial y} \\[2ex] 0 & v_x\dfrac{\partial}{\partial x}+v_y\dfrac{\partial}{\partial y} & v_x\dfrac{\partial}{\partial y} \end{bmatrix}\begin{Bmatrix} w \\ \theta_x \\ \theta_y \end{Bmatrix} = \begin{Bmatrix} v_x\,\gamma^{\varepsilon}_{xzo}+v_y\,\gamma^{\varepsilon}_{yzo} \\[1ex] v_x\,\kappa^{\varepsilon}_{xo}+v_y\,\kappa^{\varepsilon}_{xyo} \\[1ex] v_x\,\kappa^{\varepsilon}_{xyo}+v_y\,\kappa^{\varepsilon}_{yo} \end{Bmatrix} \quad \text{on } C_{\varepsilon} \tag{18.3}$$

3. BENDING OF A RECTANGULAR PLATE: A DIRECT PROBLEM

In this section, a simple plate-bending problem is considered in order to demonstrate how the inverse formulation field equations, Eqs. (17)-(18), lead to the reconstruction of the displacement solution consistent with the measured strain data. The exact strains are computed from the direct problem and are used to represent the $(\bullet)^{\varepsilon}$-strains, i.e., the measured strain data.

Consider a direct (forward) problem of a rectangular plate bent under the action of the distributed transverse loading, q(x,y). According to first-order shear-deformation plate theory,

10

the equilibrium (Euler) equations for a linearly elastic orthotropic plate have the form

$$
\left|
\begin{array}{ccc}
-G_{55}\dfrac{\partial}{\partial x} & (D_{12}+D_{66})\dfrac{\partial^2}{\partial x\,\partial y} & D_{11}\dfrac{\partial^2}{\partial x^2}+D_{66}\dfrac{\partial^2}{\partial y^2}-G_{55} \\[2ex]
-G_{44}\dfrac{\partial}{\partial y} & D_{22}\dfrac{\partial^2}{\partial y^2}+D_{66}\dfrac{\partial^2}{\partial x^2}-G_{44} & (D_{12}+D_{66})\dfrac{\partial^2}{\partial x\,\partial y} \\[2ex]
G_{55}\dfrac{\partial^2}{\partial x^2}+G_{44}\dfrac{\partial^2}{\partial y^2} & G_{44}\dfrac{\partial}{\partial y} & G_{55}\dfrac{\partial}{\partial x}
\end{array}
\right|
\left\{
\begin{array}{c} w \\ \theta_x \\ \theta_y \end{array}
\right\}
=
\left\{
\begin{array}{c} 0 \\ 0 \\ -q(x,y) \end{array}
\right\}
$$

on A (19)

where D_{ij} and G_{ij} denote, respectively, the bending and transverse shear elastic stiffness coefficients of the plate constitutive relations. Assuming that the principal material directions are coincident with the Cartesian axes, the constitutive equations express the bending moments in terms of the curvatures as,

$$
\left\{
\begin{array}{c} M_x \\ M_y \\ M_{xy} \end{array}
\right\}
=
\left[
\begin{array}{ccc}
D_{11} & D_{12} & 0 \\
D_{12} & D_{22} & 0 \\
0 & 0 & D_{66}
\end{array}
\right]
\left\{
\begin{array}{c} \kappa_{x0} \\ \kappa_{y0} \\ \kappa_{xy0} \end{array}
\right\}
\tag{20}
$$

and the transverse shear forces in terms of the transverse shear strains as

$$
\left\{
\begin{array}{c} Q_x \\ Q_y \end{array}
\right\}
=
\left|
\begin{array}{cc}
G_{55} & 0 \\
0 & G_{44}
\end{array}
\right|
\left\{
\begin{array}{c} \gamma_{xz0} \\ \gamma_{yz0} \end{array}
\right\}.
\tag{21}
$$

For a simply-supported rectangular plate of thickness $2t$ with the lateral dimensions a and b ($x \in [0,a]$, $y \in [0,b]$), that is subjected to the sinusoidal transverse loading (refer to Figure 3),

$$
q(x,y) = q_0 \sin(\alpha x)\sin(\beta y) \quad (\alpha = \pi/\text{a}, \ \beta = \pi/\text{b})
\tag{22}
$$

defined positive when acting in the positive z-direction, the exact distributions of the displacement variables are given by the trigonometric functions

$$
w = W_0 \sin(\alpha x)\sin(\beta y), \quad \theta_x = \Theta_{x0}\sin(\alpha x)\cos(\beta y), \quad \theta_y = \Theta_{y0}\cos(\alpha x)\sin(\beta y)
\tag{23}
$$

where W_0, Θ_{x0}, and Θ_{y0} define the constant amplitudes of these variables. These solutions satisfy exactly the simply-supported edge boundary conditions of the plate

Along the edges $x = 0$, a: $w = \theta_x = M_x \equiv D_{11}\theta_{y,x} + D_{12}\theta_{x,y} = 0$

Along the edges $y = 0$, b: $w = \theta_y = M_y \equiv D_{12}\theta_{y,x} + D_{22}\theta_{x,y} = 0$ (24)

The substitution of Eqs.(22)and (23) into Eqs. (19) yields a system of algebraic equations from which the values of the amplitudes W_0, Θ_{x0}, and Θ_{y0} are readily determined. This system of equations takes on the form

$$\begin{vmatrix} \alpha G_{55} & \alpha\beta(D_{12}+D_{66}) & a^2 D_{11}+\beta^2 D_{66}+G_{55} \\ \beta G_{44} & \beta^2 D_{22}+\alpha^2 D_{66}+G_{44} & \alpha\beta(D_{12}+D_{66}) \\ \alpha^2 G_{55}+\beta^2 G_{44} & \beta G_{44} & \alpha G_{55} \end{vmatrix} \begin{bmatrix} W_0 \\ \Theta_{x0} \\ \Theta_{y0} \end{bmatrix} = \begin{Bmatrix} 0 \\ 0 \\ -q_0 \end{Bmatrix} \qquad (25)$$

The above system is easily solved in terms of the unknown amplitudes. The exact expressions for W_0, Θ_{x0}, and Θ_{y0} need not be stated explicitly. Henceforth, these amplitudes will be regarded as the exact values satisfying Eqs. (25).

4. BENDING OF A RECTANGULAR PLATE: AN INVERSE PROBLEM

The field equations of the inverse bending formulation are solved herein using the strain measures derived from the exact displacement solution of the direct problem, i.e., by introducing Eqs. (23) into Eqs. (4) and (5). These strains will be used to represent the $(\bullet)^\varepsilon$-strains, i.e.,

$$\begin{Bmatrix} \kappa_{x0} \\ \kappa_{y0} \\ \kappa_{xy0} \end{Bmatrix}^\varepsilon = \begin{Bmatrix} -\alpha\Theta_{y0}\sin(\alpha x)\sin(\beta y) \\ -\beta\Theta_{x0}\sin(\alpha x)\sin(\beta y) \\ (\alpha\Theta_{x0}+\beta\Theta_{y0})\cos(\alpha x)\cos(\beta y) \end{Bmatrix}$$

$$(26)$$

$$\begin{Bmatrix} \gamma_{xz0} \\ \gamma_{yz0} \end{Bmatrix}^\varepsilon = \begin{Bmatrix} (\alpha W_0+\Theta_{y0})\cos(\alpha x)\sin(\beta y) \\ (\beta W_0+\Theta_{x0})\sin(\alpha x)\cos(\beta y) \end{Bmatrix}$$

The displacement field of the inverse solution is assumed to have the trigonometric form

$$w = W_I \sin(\alpha x)\sin(\beta y),\ \theta_x = \Theta_{xI}\sin(\alpha x)\cos(\beta y),\ \theta_y = \Theta_{yI}\cos(\alpha x)\sin(\beta y) \qquad (27)$$

where W_I, Θ_{xI}, and Θ_{yI} define the constant amplitudes of the displacement variables. The above displacement assumptions satisfy exactly the simply-supported edge boundary conditions consistent with the inverse formulation, Eqs. (18.2, 3),

Along the edges $x=0,\ a$ $(v_x=1, v_y=0)$: $w=\theta_x=\kappa_{x0}=0$
Along the edges $y=0,\ b$ $(v_x=0, v_y=1)$: $w=\theta_y=\kappa_{y0}=0$ $\qquad (28)$

12

Substituting Eqs. (26) and (27) into Eqs. (18.1), after straightforward algebraic manipulations, results in the system of equations

$$
\begin{vmatrix}
\alpha^2 + \beta^2 & \beta & \alpha \\
\lambda\beta/A & \alpha^2 + \beta^2 + \lambda/A & \alpha\beta \\
\lambda\alpha/A & \alpha\beta & \alpha^2 + \beta^2 + \lambda/A
\end{vmatrix}
\begin{Bmatrix}
W_I - W_0 \\
\Theta_{xI} - \Theta_{x0} \\
\Theta_{yI} - \Theta_{y0}
\end{Bmatrix}
=
\begin{Bmatrix}
0 \\
0 \\
0
\end{Bmatrix}
\tag{29}
$$

Equations (29) have a trivial solution for the unknown vector resulting in,

$$
\begin{Bmatrix}
W_I \\
\Theta_{xI} \\
\Theta_{yI}
\end{Bmatrix}
=
\begin{Bmatrix}
W_0 \\
\Theta_{x0} \\
\Theta_{y0}
\end{Bmatrix}
\tag{30}
$$

showing that the inverse formulation reconstructs the exact displacement field of the direct problem precisely.

5. REMARKS ON RANGE OF APPLICABILITY AND FINITE ELEMENT METHOD

The range of applicability of this formulation spans both linear and geometrically nonlinear deformation regimes, where the latter can be addressed by way of alternative formulations. For example, nonlinear strain-displacement relations can be used instead of the linear ones or, alternatively, an incremental linear analysis can be undertaken to model the large displacement response. The error functional and the corresponding relations are also readily reducible to the special cases of Timoshenko as well as the classical (Bernoulli-Euler) beam deformations.

The least-squares error functional in Eq. (9) can be used to develop displacement-based finite element methods. The finite element discretization of the error functional is closely related to formulating plate and shell (as well as beam) finite elements based upon first-order shear-deformation theory. Since the highest order derivatives in the error functional are of order one, the kinematic variables need not exceed C^0-continuity (smoothness). Thus robust and computationally efficient discretizations can be constructed. Relevant formulations of this type have already been developed for linear and nonlinear plate and shell analyses, for example, in [18-20].

6. CONCLUSIONS

A variational principle was introduced to solve the inverse problem of reconstructing the three-dimensional deformations in plate and flat shell structures using discrete strain measurements. The least squares variational principle was formulated with the use of the complete set of strain measures consistent with first-order shear-deformation theory. Euler equations and consistent boundary conditions were derived from the variational principle. The methodology does not require elastic or inertial material properties. It was demonstrated on a plate-bending problem that the inverse formulation reconstructs the exact displacement response of a direct (forward) problem once the exact strains are used to represent measured strains. The appeal of the

13

formulation is its perfect suitability for formulating C^0-continuous displacement finite elements. With the full power of the finite element method, it will be possible to apply the robust algorithms to real-time structural health monitoring applications of high-fidelity aeronautical structures.

A forthcoming report will address the inverse finite element formulation, its implementation in a general-purpose finite element code, and computational and experimental validation.

REFERENCES

1. Chang, F-K. (ed.) (2001). *Structural Health Monitoring: The Demands and Challenges.* Proceedings of Third International Workshop on Structural Health Monitoring, Stanford, California.

2. Balageas, D. L. (ed.) (2002). *Structural Health Monitoring.* Proceedings of First European Workshop on Structural Health Monitoring, Cachan (Paris), France.

3. Tikhonov, A. V. and Arsenin, V. Y. (1977). *Solutions of Ill-posed Problems.* Winston, Washington, D.C.

4. Schnur, D. S. and Zabaras, N. (1990). Finite Element Solution of Two-Dimensional Inverse Elastic Problems Using Spatial Smoothing. International Journal for Numerical Methods in Engineering, Vol. 30, pp. 57-75.

5. Maniatty, A., Zabaras, N., and Stelson, K. (1989). Finite Element Analysis of Some Inverse Elasticity Problems. Journal of Engineering Mechanics, Vol. 115, pp. 1303-1317.

6. Maniatty, A. M. and Zabaras, N. J. (1994). Investigation of Regularization Parameters and Error Estimating in Inverse Elasticity Problems. International Journal for Numerical Methods in Engineering, Vol. 37, pp. 1039-1052.

7. Liu, P-L. and Lin, H-T. (1996). Direct Identification of Non-uniform Beams Using Static Strains. International Journal of Solids and Structures, Vol. 33, No. 19, pp. 2775-2787.

8. Bogert, P. B., Haugse, E. D., and Gehrki, R. E. (2003). Structural Shape Identification from Experimental Strains using a Modal Transformation Technique. Proceedings of 44th AIAA/ASME/ASCE/AHS Structures, Structural Dynamics, and Materials Conference, AIAA 2003-1626, Norfolk, Virginia.

9. Jones, R. T., Bellemore, D. G., Berkoff, T. A., Sirkis, J. S., Davis, M. A., Putnam, M. A., Friebele, E. J., and Kersey, A. D. (1998). Determination of Cantilever Plate Shapes Using Wavelength Division Multiplexed Fiber Bragg Grating Sensors and a Least-Squares Strain-Fitting Algorithm. Smart Materials and Structures, Vol. 7, pp. 178-188.

10. Shkarayev, S., Krashantisa, R., and Tessler, A. (2001). An Inverse Interpolation Method Utilizing In-Flight Strain Measurements for Determining Loads and Structural Response of Aerospace Vehicles. Proceedings of Third International Workshop on Structural Health Monitoring, Stanford, California, pp. 336-343.

11. Shkarayev, S., Raman, A., and Tessler, A. (2002). Computational and Experimental Validation Enabling a Viable In-Flight Structural Health Monitoring Technology. Proceedings of First European Workshop on Structural Health Monitoring, Cachan (Paris), France.

12. Reissner, E. (1944). On the Theory of Bending of Elastic Plates. J. Math. Physics, Vol. 23, pp. 184-191.

13. Reissner, E. (1945). The Effect of Transverse Shear Deformations on the Bending of Elastic Plates. J. Applied Mechanics, ASME, Vol. 12, pp. A69-A77.

14. Mindlin, R. D. (1951). Reflections on the Theory of Elastic Plates. Applied Mechanics Review, Vol. 38, pp. 1453-1464.

15. Lancaster, P. and Salkauskas, K. (1986). *Curve and Surface Fitting: An Introduction.* Academic Press, London.

16. Tessler, A., Riggs, H. R., Freese, C. E., and Cook, G. M. (1998). An Improved Variational Method for Finite Element Stress Recovery and a Posteriori Error Estimation. Computer Methods in Applied Mechanics and Engineering, Vol. 155, pp. 15-30.

17. Tessler, A., Riggs, H. R., and Dambach, M. (1999). A Novel Four-Node Quadrilateral Smoothing Element for Stress Enhancement and Error Estimation. International Journal for Numerical Methods in Engineering, Vol. 44, pp. 1527-1543.

18. Tessler, A., and Hughes, T. J. R. (1985). A Three-Node Mindlin Plate Element with Improved Transverse Shear. Computer Methods in Applied Mechanics and Engineering, Vol. 50, pp. 71-101.

19. Tessler, A. (1990). A C^0-Anisoparametric Three-Node Shallow Shell Element. Computer Methods in Applied Mechanics and Engineering, Vol. 78, pp. 89-103.

20. Barut, A., Madenci, E., and Tessler, A. (1997). Nonlinear Analysis of Laminates Through a Mindlin-type Shear Deformable Shallow Shell Element. Computer Methods in Applied Mechanics and Engineering, Vol. 143, pp. 155-173.
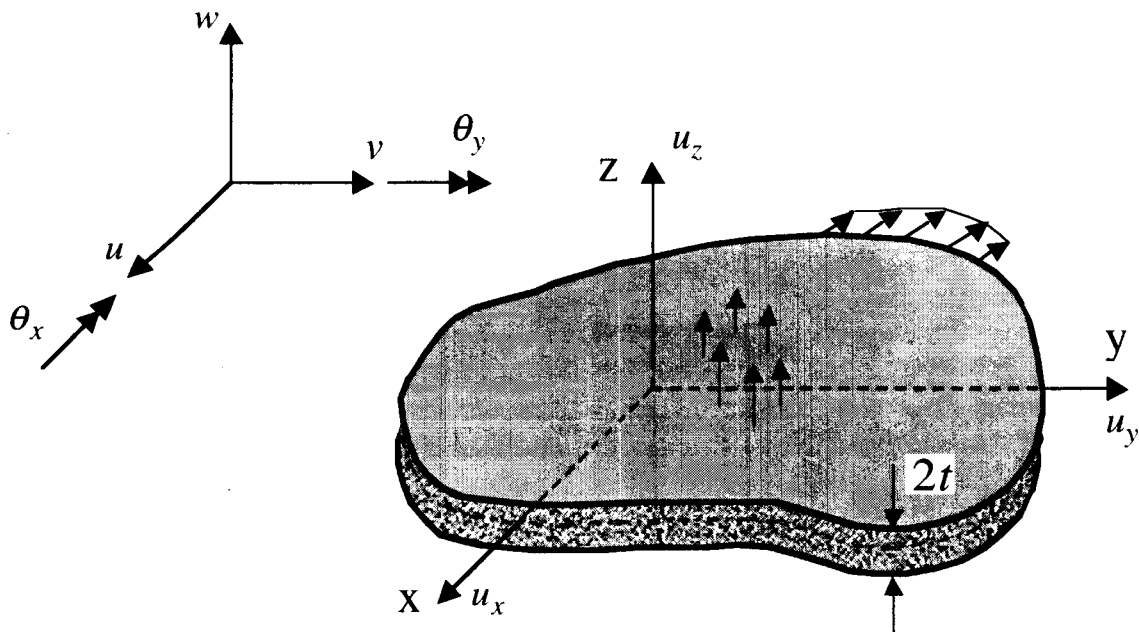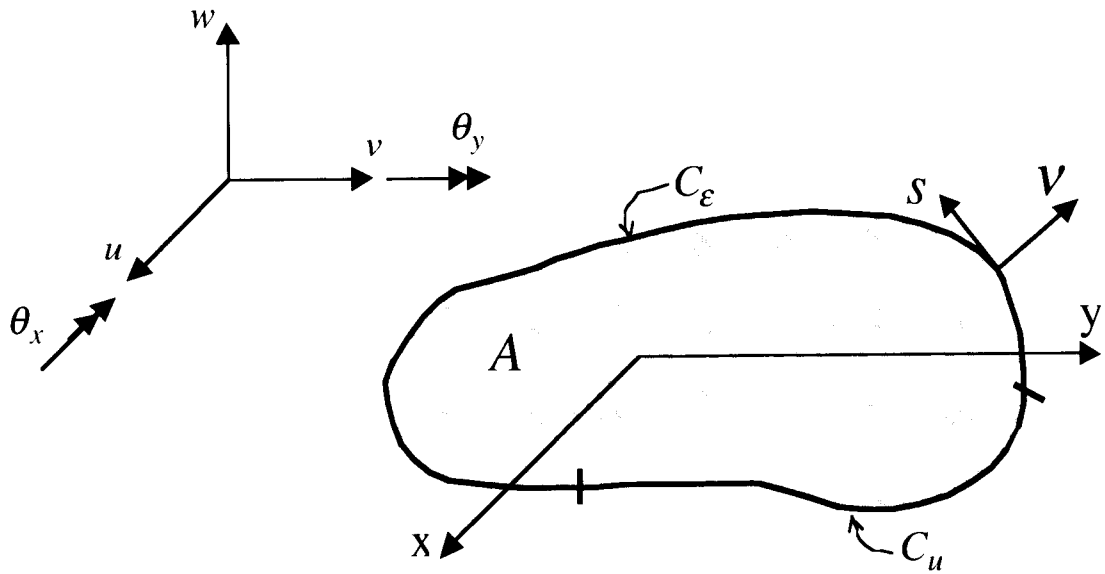
Figure 1. Notation for the flat shell.

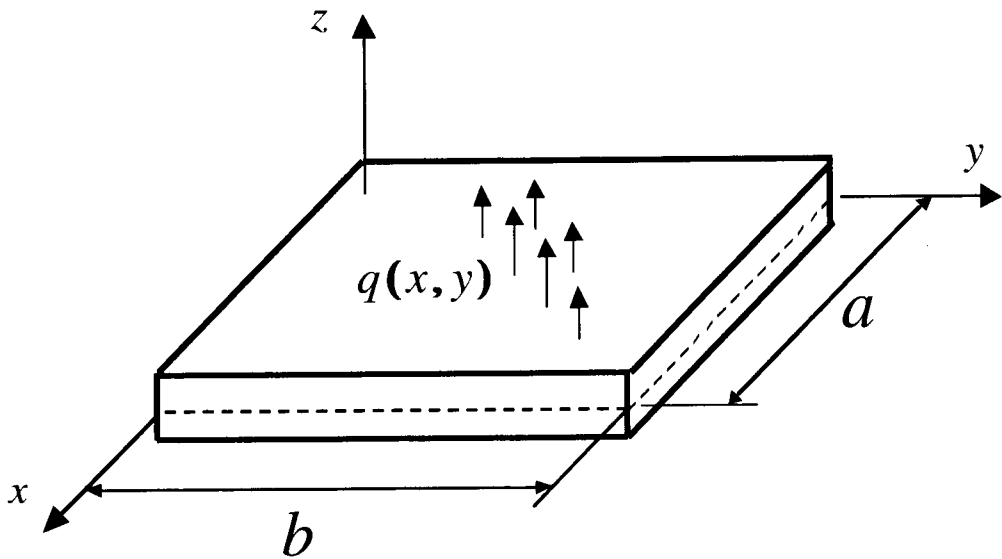Figure 2. Notation for the shell middle plane.

Figure 3. Simply-supported rectangular plate under sinusoidal transverse loading.

REPORT DOCUMENTATION PAGE		Form Approved OMB No. 0704-0188

The public reporting burden for this collection of information is estimated to average 1 hour per response, including the time for reviewing instructions, searching existing data sources, gathering and maintaining the data needed, and completing and reviewing the collection of information. Send comments regarding this burden estimate or any other aspect of this collection of information, including suggestions for reducing this burden, to Department of Defense, Washington Headquarters Services, Directorate for Information Operations and Reports (0704-0188), 1215 Jefferson Davis Highway, Suite 1204, Arlington, VA 22202-4302. Respondents should be aware that notwithstanding any other provision of law, no person shall be subject to any penalty for failing to comply with a collection of information if it does not display a currently valid OMB control number.
PLEASE DO NOT RETURN YOUR FORM TO THE ABOVE ADDRESS.

1. REPORT DATE *(DD-MM-YYYY)* 01- 08 - 2003	2. REPORT TYPE Technical Memorandum	3. DATES COVERED *(From - To)*

4. TITLE AND SUBTITLE A Variational Principle for Reconstruction of Elastic Deformations in Shear Deformable Plates and Shells	5a. CONTRACT NUMBER
	5b. GRANT NUMBER
	5c. PROGRAM ELEMENT NUMBER
6. AUTHOR(S) Tessler, Alexander; and Spangler, Jan L.	5d. PROJECT NUMBER
	5e. TASK NUMBER
	5f. WORK UNIT NUMBER 23-755-06-00

7. PERFORMING ORGANIZATION NAME(S) AND ADDRESS(ES) NASA Langley Research Center Hampton, VA 23681-2199	8. PERFORMING ORGANIZATION REPORT NUMBER L-19000

9. SPONSORING/MONITORING AGENCY NAME(S) AND ADDRESS(ES) National Aeronautics and Space Administration Washington, DC 20546-0001	10. SPONSOR/MONITOR'S ACRONYM(S) NASA
	11. SPONSOR/MONITOR'S REPORT NUMBER(S) NASA/TM-2003-212445

12. DISTRIBUTION/AVAILABILITY STATEMENT
Unclassified - Unlimited
Subject Category 39
Availability: NASA CASI (301) 621-0390   Distribution: Standard

13. SUPPLEMENTARY NOTES
Tessler: Langley Research Center; Spangler: Lockheed Martin Aeronautics Company
An electronic version can be found at http://techreports.larc.nasa.gov/ltrs/ or http://ntrs.nasa.gov

14. ABSTRACT
A variational principle is formulated for the inverse problem of full-field reconstruction of three-dimensional plate/shell deformations from experimentally measured surface strains. The formulation is based upon the minimization of a least squares functional that uses the complete set of strain measures consistent with linear, first-order shear-deformation theory. The formulation, which accommodates for transverse shear deformation, is applicable for the analysis of thin and moderately thick plate and shell structures. The main benefit of the variational principle is that it is well suited for C0-continuous displacement finite element discretizations, thus enabling the development of robust algorithms for application to complex civil and aeronautical structures. The methodology is especially aimed at the next generation of aerospace vehicles for use in real-time structural health monitoring systems.

15. SUBJECT TERMS
finite element method; inverse problem; least squares; plates and shells; shear deformation theory; variational principle

16. SECURITY CLASSIFICATION OF:			17. LIMITATION OF ABSTRACT	18. NUMBER OF PAGES	19a. NAME OF RESPONSIBLE PERSON
a. REPORT	b. ABSTRACT	c. THIS PAGE			STI Help Desk (email: help@sti.nasa.gov)
					19b. TELEPHONE NUMBER *(Include area code)*
U	U	U	UU	21	(301) 621-0390

Standard Form 298 (Rev. 8-98)
Prescribed by ANSI Std. Z39.18